Fuel 333 (2023) 126519

Contents lists available at ScienceDirect

Fuel

journal homepage: www.elsevier.com/locate/fuel

Full Length Article

Predictive modelling and optimization of performance and emissions of an auto-ignited heavy naphtha/*n*-heptane fueled HCCI engine using RSM

Tolga Kocakulak [a,*], Serdar Halis [b], Seyed Mohammad Safieddin Ardebili [c], Mustafa Babagiray [d], Can Haşimoğlu [e], Masoud Rabeti [f], Alper Calam [g]

[a] Burdur Mehmet Akif Ersoy University, Vocational High School of Technical Sciences, Burdur, Turkey
[b] Automotive Engineering Department, Faculty of Technology, Pamukkale University, Denizli, Turkey
[c] Department of Biosystems Engineering, Shahid Chamran University of Ahvaz, Ahvaz, Iran
[d] Mechanical Engineering Department, Hamburg University of Technology, Hamburg, Germany
[e] Mechanical Engineering, Faculty of Technology, Sakarya University of Applied Science, Sakarya, Turkey
[f] Department of Mechanical Engineering, Sousangerd Branch, Islamic Azad University, Sousangerd, Iran
[g] Gazi University, Technical Sciences Vocational High School, Ostim, Ankara, Turkey

ARTICLE INFO

Keywords:
HCCI engine
Heavy naphtha
Optimization approach
Response surface methodology

ABSTRACT

In this study, the effects of engine speed and lambda input parameters of a single-cylinder HCCI engine on the performance, combustion and emissions with the use of fuels with different concentrations were investigated. As finding of the best operating point of the engine perfomance is vital, therefore, in this research work the Response Surface Method waas used to model and optimize the process. The processes of determining the experimental sets, creating the model equations of the response parameters and performing the optimization were carried out with the RSM method. The engine speed was determined as 800–1600 rpm, the lambda value was 1.8–2.6 and the naphtha ratio in the mixed fuel was 0–100 %. As a result of the study, ANOVA tables, model equations, contour graphics of response parameters were created and the effects of input parameters were examined in detail. The accuracy of the model equations created by comparing the estimated and actual response parameter values has been strengthened. After the optimization, the optimum input parameters were calculated as 75 % naphtha ratio, 1166.75 rpm engine speed and 2.12 lambda value. The response parameter values obtained depending on the optimum input parameters are effective torque 6.26 Nm, indicated thermal efficiency 33.09 %, BSFC 196.79 g/kWh, CA10 0.77 °CA, CA50 5.6 °CA, combustion duration 28.84 °CA, COV_{imep} 1.46 %, MPRR It was determined as 6.24 bar/°CA, UHC 375.96 ppm and CO 0.05 %.

1. Introduction

Industrial pollution and wastes from energy conversion plants make agricultural areas unusable and pollute the atmosphere rapidly [1–4]. Exhaust emissions caused by millions of vehicles used in the automotive industry are among the factors that threaten the atmosphere. Compression ignition (CI) engines, which are widely used in heavy-duty road vehicles, ship industry and rail systems, cause high nitrogen oxide (NOx) and soot emissions. Exhaust emissions of spark ignition (SI) engines are at more controllable levels than in CI mode. However, fuel consumption is high and thermal efficiency is low in SI mode [5–7].

Homogeneous charged compression ignition (HCCI) combustion mode has some advantages such as high thermal efficiency and low emissions, which can be an alternative to SI and CI engines [8,9]. Although electric vehicles will be widely used in the automotive industry in the future, these vehicles still have some problems to be solved. The main of these problems are charging time, battery life, range and how to supply the electrical energy needed by millions of vehicles [10,11]. Researchers predict that by the end of 2040, approximately 85 % of registered vehicles will have internal combustion engines [12]. Therefore, internal combustion engines will continue to be widely used in transportation and heavy industry facilities in the near future [13]. Energy is getting more expensive each passing day in today's world. The Brent oil prices are not stable, and its value is increasing day by day. For this reason, new combustion modes, which can be alternatives to SI and

* Corresponding author.
E-mail addresses: tkocakulak@mehmetakif.edu.tr (T. Kocakulak), shalis@pau.edu.tr (S. Halis), m.safieddin@scu.ac.ir (S.M.S. Ardebili), mustafa.babagiray@tuhh.de (M. Babagiray), canhasim@subu.edu.tr (C. Haşimoğlu), m.rabeti@iaud.ac.ir (M. Rabeti), acalam@gazi.edu.tr (A. Calam).

https://doi.org/10.1016/j.fuel.2022.126519
Received 9 May 2022; Received in revised form 11 September 2022; Accepted 25 October 2022
Available online 3 November 2022
0016-2361/

Nomenclature

ANOVA	Analysis of variance
BSFC	Brake spesific fuel consumption
CA	Crank angle
CAE10	Crank angle location of 10 % accumulated HRR (°CA)
CAE50	Crank angle location of 50 % accumulated HRR (°CA)
CAK	Crambe abyssinica KOH catalyst
CAN	Crambe abyssinica NaOH catalyst
CI	Compression ignition
CO	Carbon monoxite
CO_2	Carbon dioxite
COV_{imep}	cyclical differences
F30	30 % fusel oil and 70 % *n*-heptane
HCCI	Homogeneous charged compression ignition
h_g	convection and heat transfer coefficient
IMEP	Indicated mean effective pressure
ITE	Indicated thermal efficiency
LPG	Liquid petroleum gas
LTC	low temperature combustion
MPRR	Maximum pressure rise rate
θ	Crank angle
NOx	Nitrogen oxide
P	In-cylinder pressure
PCCI	premixed charge compression ignition
Q	represents the lower heating value
RCCI	reactivity controlled compression ignition
RSM	response surface method
SI	spark ignition
Tw	Cylinder wall temperature
UHC	Unburned hydrocarbon
V	Cylinder value
$\overline{X}$	Standard deviation

CI engines, are expected to provide low fuel costs along with emission and efficiency advantages [14].

HCCI engines are in the low temperature combustion (LTC) cycle group together with premixed charge compression ignition (PCCI) and reactivity controlled compression ignition (RCCI) engines. In all three combustion models, the maximum in-cylinder temperatures are low, so NOx emissions are almost zero without the use of an additional exhaust after-treatment system. In addition, oxidation reactions occur very quickly in LTC modes and accordingly, heat losses from the cylinder wall are reduced. Thus, the thermal efficiency increases [15,16]. Despite these advantages of LTC combustion mode, the use of liquid and gas phase fuels is mandatory in PCCI and RCCI engines. Combustion phase is tried to be controlled by making use of different physical and chemical properties of fuels. In particular, NOx and soot emissions are reduced. However, it is an important disadvantage that the use of fuels with different properties creates the need for two different fuel systems and the need for a specific software to control these systems. Because it is very difficult to determine which fuel will be injected in which position of the crankshaft, in how long and in how much [17–19]. HCCI engines are not dependent on the fuel to be used and HCCI combustion can be achieved with a single fuel in the liquid or gas phase. The air fuel mixture can be prepared by port injection or early direct injection. In addition, HCCI combustion can be obtained with ultra-lean mixtures at suitable operating conditions. Thus, high thermal efficiency can be achieved with low fuel consumption [20,21]. In addition to these advantages, the HCCI mode also has some problems that need to be resolved. The operating range in HCCI combustion is narrow. There is no physical mechanism that controls the start of combustion and the combustion process. Moreover, there is knocking at high loads and misfire at low loads [22,23]. Combustion must be slowed down so that knock can be reduced. For this, methods such as variable valve timing and exhaust gas recirculation can be used [24,25]. In order to overcome the misfire problem, the intake air can be heated or the compression ratio increased [26,27]. However, these methods are not sufficient to control the combustion process. In addition to these methods, the physical and chemical properties of the fuel used also significantly affect the HCCI combustion phase [14]. While low reactivity (gasoline, ethanol, methanol etc.) fuels can be preferred to eliminate the knocking problem, high reactivity (diesel, biodiesel, diethyl ether, dimethyl ether etc.) fuels can solve the misfire problem [16]. The ideal octane or cetane number of the fuel to be used in HCCI combustion mode varies depending on the compression ratio of the engine [28,29]. Calam et al. [26] performed an experimental study to determine the ideal fuel reactivity at different compression ratios in an HCCI engine. It has been stated that while the optimum operating range is provided with RON20 fuel in conditions where the compression ratio is 10, the widest operating range is obtained with RON40 fuel by increasing the compression ratio to 11. However, the reactivity of the fuel is not the only parameter that affects the oxidation reactions. The properties of fuel such as latent heat of evaporation, density and viscosity are also very important in order to prepare the mixture homogeneously in HCCI mode. In addition, the preferred fuel should not be costly and should be easily available [14].

In order to have information about whether a fuel type is suitable for the HCCI mode and the performance of that fuel, the boundary conditions of the operation should be determined. For this reason, many experiments are required to determine the optimum fuel type and operating conditions in HCCI engines. In this type of tests, analysis can also be made by mixing the test fuel to be used with reference fuels (*n*-heptane, isooctane etc.) in various proportions. In this case, the number of tests increases even more, causing researchers to lose a lot of time [30,31]. Various optimization methods can be preferred to eliminate this problem. Thus, the optimum test fuel that solves HCCI problems can be determined and combustion analysis can be performed. In recent years, researchers working in the field of internal combustion engine technology have preferred the response surface method (RSM), which enables them to make predictions with high accuracy [32–36]. In the RSM, the variables to be preferred in the experimental study are defined to a computer interface program. These variables may include fuel mixture ratios as well as engine operating parameters. The computer interface program shows how many test points should be recorded depending on the number of variables with the preliminary analysis performed. At these conditions, engine tests are performed and results including outputs such as torque, fuel consumption, power, start of combustion, combustion duration, thermal efficiency, pressure rise rate, the coefficient of variation in the indicated mean effective pressure (IMEP) and emissions are recorded for each fuel type in the interface program. As a result of the optimization process, estimations can be made at different ratios for the mixture test fuels. The accuracy of the optimization is determined by comparative analysis of the experimental and predicted results [37–39].

Simsek et al. [40] used the RSM method to determine optimum operating conditions in a gasoline-LPG dual-fueled SI engine. In this study, which only 15 data points were used for the optimization process, it was determined that the ideal LPG ratio was 35 % with a 4 % margin error. Khanjani et al. [41] analyzed the effects of water-waste fish oil biodiesel-diesel ternary fuel mixture and various ratios of surfactants on engine performance and emissions in a CI engine with the RSM method. In the optimization process performed with 17 data points, it was determined that the ideal mixture for full load and 1800 rpm engine

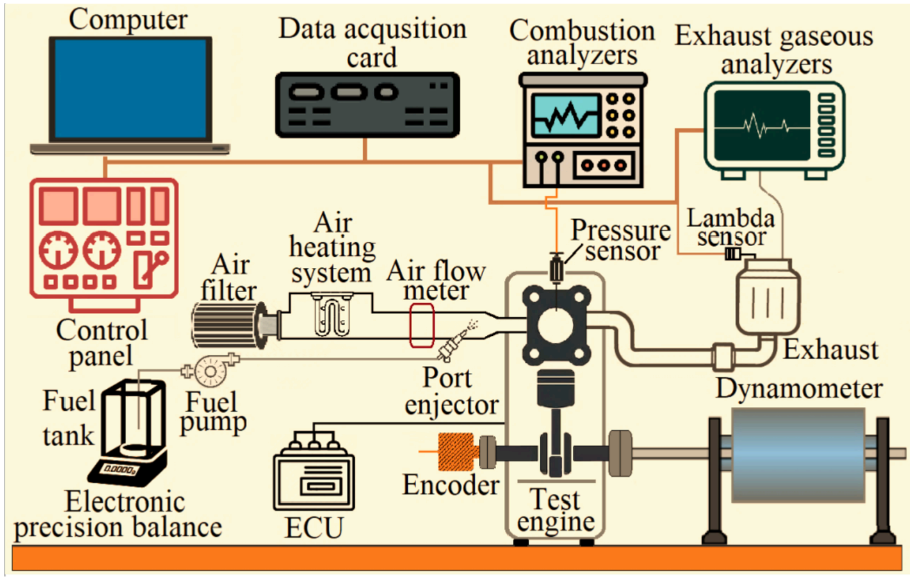

Fig. 1. Schematic representation of experimental test setup.

speed was 6.13 % water, 3 % biodiesel, 1 % surfactant and the remainder was diesel fuel. Srinidhi et al. [42] used the RSM method to determine the optimum nickel oxide (NiO) additive to be added to B25 (neem biodiesel 25 %+diesel 75 %) fuel. This experimental study was carried out at 1500 rpm engine speed and full load conditions. The start of injection, injection pressure and compression ratio were changed to determine the optimum operating conditions. Data were recorded from 29 different test points and the optimization process was applied. The results show that the most ideal fuel mixture is obtained with the addition of 25 ppm NiO to B25 fuel. It was stated that the most suitable operating conditions for this test fuel were the start of injection at 26.998 °CA bTDC, injection pressure of 227.86 bar and compression ratio of 17.2585:1. These numerical values were obtained with an average margin error of 2.37 %. The RSM method has been validated in a few studies in the literature to determine the combustion characteristics of HCCI engines. A detailed optimization study for HCCI combustion was carried out for the first time in the literature by Ardebili et al. [37]. The effect of fusel oil-diethyl ether mixture fuels in various ratios on HCCI combustion was analyzed by the RSM method under different operating conditions. The optimum fuel mixture and operating conditions were determined for three different fuels, three different lambda values, and three different engine speeds by using only 17 test points. The results of this study show that the ideal test fuel for HCCI combustion is a mixture of 41.72 % diethyl ether + 58.28 % fusel oil with 82 % accuracy. It was expressed that torque of 11.80 Nm, cyclical differences (COV_{imep}) of 1.36 %, the maximum pressure rise rate (MPRR) of 3.14, the brake specific fuel consumption (BSFC) of 268 g/kWh, the start of combustion at 7.52 °CA and CA50 at 11 °CA data were predicted by using this fuel mixture with high accuracy at an engine speed of 882 rpm and 2.08 lambda conditions in HCCI mode. Kocakulak et al. [39] investigated the optimum operating conditions of fusel oil-*n*-heptane fuel mixtures in HCCI engines. Optimization was carried out with RSM method for engine speed, lambda and fuel mixture ratio parameters. Optimization results show that the ideal fuel mixture ratio is 30 % fusel oil and 70 % *n*-heptane (F30) for optimum HCCI combustion between knock and misfire limits and minimum emissions. The indicated thermal efficiency (ITE) was 34 % at 1260 rpm engine speed and at 1,91 lambda value by using F30 fuel. In addition, NOx emissions are almost zero under these conditions. Babagiray et al. [43] optimized the effects of different valve lift heights, engine speed, lambda values and intake air temperatures on HCCI combustion using reference RON80 fuel. The ideal HCCI operating conditions were obtained with 5.5 mm intake lift height, 3.5 mm exhaust lift height, 1168.82 rpm engine speed, 0.971 lambda value and 100.07 °C intake air temperature. Atmanlı et al. performed the optimization of *n*-butanol-diesel and cotton oil fueled diesel engine with RSM. According to the results, they observed that butanol reduces the braking torque compared to diesel fuel. They also observed that adding butanol to diesel fuel increased fuel consumption by 24.53 % [32].

Naphtha fuels with low octane and cetane number have been a source of interest in studies in low temperature combustion mode. Different researchers have carried out studies that achieved low NOx and soot emissions without significant changes in engine equipment [44–47]. Naphtha fuels from crude oil can be produced with less processing during the production of gasoline. Naphtha fuels require less distillation processing of petroleum, less energy consumption for their production. They are promising for engines with low temperature combustion mode due to their fuel properties. This study has two different features from the studies in the literature. First of all, it is seen that heavy naphtha fuel has not been investigated in detail in solving the problems of HCCI engines. In addition, the use of heavy naphtha fuel mixtures in various ratios could expand the operating ranges. Secondly, determining the optimum mixing ratio with RSM in order to achieve optimum combustion characteristics, performance and emission values will bring a novelty to the literature with this study.

In this study, the effects of mixed fuels formed with *n*-heptane and naphtha on combustion, performance and emissions were investigated using experimental and statistical methods in a HCCI engine. Naphtha ratio, engine speed and lambda value were taken as input parameters. For response parameters, effective torque, Indicated thermal efficiency, BSFC, CA10, CA50, combustion duration, COV_{imep}, MPRR, unburned hydrocarbon (UHC) and carbon monoxite (CO) values were investigated. There are some studies carried out in the literature with high accuracy on the control of the combustion phase in hcci engines with the RSM method [37,39].

2. Materials and methods

The results obtained in this study were carried out using experimental, numerical and statistical methods. Experimental processes were carried out on the test setup. The data obtained with the experimental method were analyzed numerically in the MATLAB environment. Determining the experimental sets, obtaining the equations used for the estimation of the response parameters depending on the input

Table 1
Test engine datas.

Brand-Model	Ricardo Hydra
Bore × Stroke	80.26 mm × 88.90 mm
Compression ratio	5:1–13:1
Maximum power	15 kW @ 4500 rpm
Maximum speed	5400 rpm
Maximum cylinder pressure	120 bar

Table 2
The accuracies of the measured values and the uncertainty analysis in the results.

	Uncertainties [%]	Accuracy
Test fuels [g]	±0.22	±0.001 [g]
Engine speed [rpm]	±1	±1 [%]
Torque [Nm]	±0.24	±0.20 [%]
In-cylinder pressure [bar]	±1.63	±0.5 [bar]
Indicated thermal efficiency [%]	±1.32	–
IMEP [bar]	±1.75	–
COV_{imep} [%]	±1.94	–
CA10 [CA]	±1.25	–
CA50 [CA]	±1.25	–
CO [% vol]	±1.7	±0,001
UHC [ppm]	±1.34	±1
NO [ppm]	±0.5	±1
Lambda	±1.85	±0,001

parameters, and making the optimization were carried out with the help of Design experimenter 11. The methods and processes used in the study are mentioned in detail in this section.

2.1. Experimental test setup

The experimental processes carried out in this study were carried out with a test setup with an internal combustion engine that can be operated in HCCI mode. There are internal combustion engine, encoder, in-cylinder pressure sensor, dynamometer, combustion analyzer, data acquisition card, control panel, precision balance, fuel tank and pump, air filter, air heating system, lambda sensor and exhaust gas analyzer on the test setup. The schematic view of the test setup in which the experimental study was carried out is given in Fig. 1.

In the experimental setup, a single cylinder, 450 cc volume, Ricardo Hydra model, port type fuel and liquid cooling system, compression ratio adjustable internal combustion engine was used. The technical datas of the internal combustion engine are given in Table 1.

The internal combustion engine has a naturally aspirated air system, and the air taken from the atmosphere is filtered, the temperature is controlled, the amount is measured and sent to the intake port. The measurement of the fuel stored in the tank is carried out with a precision balance of 0.01 g. The measured fuel is pressurized by the fuel pump and delivered to the injectors. Fuel is sprayed on the air taken into the intake port with an injector and the resulting filling is sent into the cylinder. By measuring the amount of air and fuel taken into the cylinder, the lambda value can be precisely controlled. McClure brand dynamometer, which can absorb a maximum of 30 kW of power, is used to control the load of the internal combustion engine.

The crankshaft position is determined with the help of the encoder, which is integrated into the engine crankshaft and reads 1000 pulses in each revolution of the crankshaft. Simultaneously, Kistler-6121 model in-cylinder pressure sensor is used. The pressure sensor used can measure between 0 and 250 bar. The operating temperature of the sensor is between 223 K and 623 K and needs liquid cooling. It is stated in the datasheet that the measurement sensitivity of the sensor is 14.7 pC/bar and the accuracy is ±<0.5 %.

The information coming from the combustion analyzer and data acquisition card is transferred to the computer environment. In addition to these, in the study, engine emission values were also examined. Emission values were measured with the help of Bosch BEA350 exhaust gas analyzer. Table 2 shows the accuracy of the exhaust gas analyzer datas and uncertainty of the recorded data during experiments.

2.2. Formulas and equations

The response parameters are obtained by numerically analyzing the data obtained in the experimental study in the MATLAB environment. The heat release rate is calculated by Equation (1). In the heat release rate equation, k is above isontropic, p is the in-cylinder pressure, V is the stroke volume, theta is the crankshaft angle, and Q_{heat} is the heat released from the cylinder walls. The in-cylinder pressure value is measured with the help of a sensor. The crankshaft position is determined by the encoder. The cylinder volume value is calculated numerically, depending on the engine structural parameters and the crankshaft position [48].

$$\frac{dQ}{d\theta} = \frac{k}{k-1} p \frac{dV}{d\theta} + \frac{k}{k-1} V \frac{dP}{d\theta} + \frac{dQ_{heat}}{d\theta} \tag{1}$$

The heat transferred from the cylinder walls to the atmosphere is calculated by Equation (2) [49]. In the equation, h_g is the convection and heat transfer coefficient, A is the area, n is the number of cylinders, T_g is the cylinder temperature, and T_w is the ambient temperature.

$$\frac{dQ_{heat}}{d\theta} = \frac{1}{6 \times n} \times h_g \times A \times \left(T_g - T_w\right) \tag{2}$$

If the pressure and volume changes of a closed system are known, the amount of work performed in that system can be determined. In this context, the amount of net work produced in the engine can be calculated by Equation (3) [43]. In the equation, dV is the change in the cylinder volume depending on the crankshaft angle, and P is the instantaneous pressure in the cylinder.

$$W_{net} = \int PdV \tag{3}$$

Thermal efficiency is obtained by dividing the net work obtained as a result of combustion to the lower calorific value of the fuel taken into the cylinder. In this study, the amounts and lower calorific values of naphtha and *n*-heptane fuels are included in the calculation, since mixed fuels are used. Equation (4) is used to determine the thermal efficiency [50,51]. In the equation, m represents the amount of fuel, and Q represents the lower heating value of the fuel.

$$\eta_T = \frac{W_{net}}{\dot{m}_{naphta} \times Q_{naphta} + \dot{m}_{n-\text{heptane}} \times Q_{n-\text{heptane}}} \tag{4}$$

The expression of the amount of fuel required for the production of one kWh of energy is provided by BSFC. The BSFC value is calculated by dividing the amount of fuel used by the net work achieved. Calculation of the BSFC value is realized by Equation (5) [52].

$$BSFC = \frac{m_f}{W_{total}} \tag{5}$$

In order to strengthen the accuracy of the response parameter values obtained during the experiments, the average of 50 cycle values is used. It is inevitable that there will be differences in the response parameter values obtained between these cycles. These deviations between cycles are defined as COV_{imep}. COV_{imep} can be calculated with the help of Equation (6). The value of $\overline{X}$ in the equation represents the standard deviation value for consecutive cycles, and σ_{imep} represents the mean cycle pressure value.

$$COV_{imep} = \frac{\sigma_{imep}}{\overline{X}} \cdot 100 \tag{6}$$

Pressure measurement in the cylinder is carried out depending on the crankshaft angle. The maximum pressure rise rate is defined as the

Table 3
Spesification of *n*-Heptane and Naphtha.

	Naphtha	*n*-Heptane
Calorific value (kJ/kg)	43,36	44,566
RON	68	0
Boiling point (°C)	152	97–98
Density (kg/cm^3 at 20 °C)	0.72	0.68
Viscosity (cSt)	0.5	0.57

maximum value of the derivative values of the in-cylinder pressure value depending on the crankshaft angle. The MPRR value is obtained by Equation (7).

$$MPRR = \left(\frac{dP}{dCA}\right)_{max} \tag{7}$$

2.3. Test fuels

In this study, mixed fuels of different concentrations were prepared using *n*-heptane and naphtha fuels and their effects on combustion, efficiency and performance on HCCI engine were investigated experimentally and statistically. The naphtha ratio in the fuel mixture was determined as 0 %, 25 %, 50 %, 75 % and 100 %. Due to the self-ignition of the filler on the HCCI engine, the operating limits can be narrow. In case of using pure *n*-heptane and pure naphtha on the engine, the engine could not be started at very high and very low effective torque and lambda values. For this reason, the focus is on blended fuels with 25 %, 50 % and 75 % naphtha ratios in the blended fuel.

Table 3 shows the calorific, RON, boiling point, density and viscosity values of pure *n*-heptane and pure naphtha fuels [31]. When the two fuels are examined, it is seen that the most striking differences between them are in RON and boiling point values. In addition, the calorific value of naphtha fuel is lower than that of *n*-heptane fuel. Although the density of *N*-heptane fuel is lower than naphtha fuel, it is seen that the viscosity value is slightly higher.

2.4. Response surface method

Internal combustion engines have different input parameters. Examining the effects of these input parameters with each other causes very high costs and time. Making improvements in terms of cost and time in such experimental studies makes the process more efficient. In order to make this improvement, the use of the response Surface Method (RSM), which is a statistical method, provides a great advantage. After obtaining the experimental set with the RSM method, numerical modeling and optimization processes are carried out [53].

The experimental parameter values made with the created numerical model provide the most accurate way to reach the response parameter values, regardless of the intermediate values and boundary conditions. Reducing the number of experiments with RSM also helps to determine the optimum input parameters depending on the targeted response outputs and the values obtained with the experimental methods [54].

The application of the RSM method is seen on the flow chart given in Fig. 2 [77]. The values including the minimum and maximum values of the input parameters that are aimed to be examined in the study should be determined. As a result of the study, the required data measurement is carried out during the experiments performed by determining the response parameters that are aimed to be examined. After the input and output parameters are determined, RSM design is made and experimental sets are created. The created experimental sets are carried out depending on the specified input parameters, provided that all conditions are the same. By transferring the experimental data to the RSM environment, graphics and model of the response parameters are created depending on the input parameters. The last step of the RSM method is optimization. Optimization is carried out by entering the targeted values in the response parameters and the optimum input parameter values are determined.

In this study, the application of the RSM method was carried out in the Design Expert 11 environment. Using Central composite design (CCD) on the program, 3 numerical factors were input. Naphtha ratio, engine speed and lambda value were taken as RSM input parameters. The minimum and maximum values of naphtha ratio, engine speed and lambda values were determined according to engine operating conditions. Values of independent parameters are shown in Table 4.

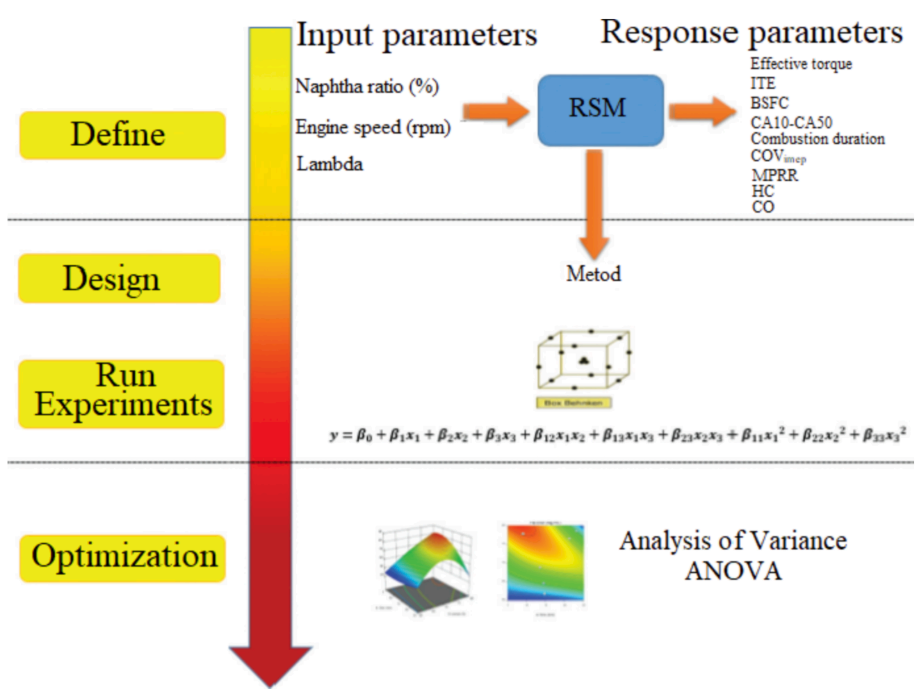

Fig. 2. RSM flow chart.

Table 4
Levels for independent variables.

Independent variables	Codes	Levels				
		$-\alpha$	-1	0	$+1$	$+\alpha$
Naphtha ratio (%)	A	0	25	50	75	100
Engine speed (rpm)	B	800	1000	1200	1400	1600
Lambda	C	1,8	2	2.2	2.4	2.6

Table 5
RSM experiment set variable input parameters.

Std	Run	Naphtha ratio (%)	Engine speed (rpm)	Lambda
2	1	75	1000	2
16	2	50	1200	2,2
18	3	50	1200	2,2
12	4	50	1600	2,2
9	5	0	1200	2,2
1	6	25	1000	2
14	7	50	1200	2,6
6	8	75	1000	2,4
13	9	50	1200	1,8
3	10	25	1400	2
17	11	50	1200	2,2
5	12	25	1000	2,4
19	13	50	1200	2,2
11	14	50	800	2,2
15	15	50	1200	2,2
8	16	75	1400	2,4
10	17	100	1200	2,2
4	18	75	1400	2
20	19	50	1200	2,2
7	20	25	1400	2,4

Analysis of variance (ANOVA) was used to evaluate the model equality created for each response parameter. The cubic model used to obtain the response parameters depending on the variable parameters entered into the RSM is given in Equation (8) [55]. In the equation, x_i is the input variable, $\hat{y}$ is the response, β_0 is the constant coefficient,β_i, β_{ii} and β_{iii} is the regression coefficient, and Bij is the Cubic coefficient.

$$\hat{y} = \beta_0 + \sum_{i=1}^{k}\beta_i x_i + \sum_{i=1}^{k}\beta_{ii}x_i^2 + \sum_{i=1}^{k}\beta_{iii}x_i^3 + \sum_{i=1}^{k}\sum_{j=1,i<j}^{k}\beta_{ij}x_i x_j \tag{8}$$

There are 20 experiments in total in the design created by RSM. The variable parameter values of the experimental set are given in Table 5.

Table 6
ANOVA results for effective torque.

Source	Sum of Squares	Mean Square	F-value	p-value	Remarks
Model	16.29	1.25	11.82	0.0031	significant
A-Naphtha ratio	9.24	9.24	87.17	< 0.0001	significant
B-Engine speed	0.045	0.045	0.4243	0.5389	Not significant
C-Lambda	0.605	0.605	5.7	0.0541	Not significant
Residual	0.6363	0.1061			
Cor Total	16.93				

results and the actual results [60]. If the difference between R^2 and Adj. R^2 value is 0.2 or less, the accuracy of the applied method is accepted [42].

3.1. Examination of combustion, performance and efficiency parameters

Examination of combustion, performance and efficiency parameters in the use of alternative fuels on an internal combustion engine is of critical importance in determining the efficiency of the fuel or fuel mixture. The effects of engine speed and lambda variable parameters on the effective torque, ITE, BSFC, CA10, CA50, COV_{imep} and MPRR of the blended fuels formed with *N*-heptane and naphtha fuels are discussed in detail.

3.1.1. Effective torque (Nm)

Effective torque is one of the most important parameters used in the calculation of engine power and required to define engine performance characteristics. ANOVA results for effective torque are given in Table 6. It was determined that engine speed and lambda values are insignificant for the effective torque value, while the naphtha ratio is important. The F-value is the ratio of the between and within variation. Generally, the higher the F- value in ANOVA the greater variation between sample means. However the higher F-value corresponds to the lower p-value (probability value). The p-value measures the evidence against the null hypothesis. Lower probabilities provide stronger evidence against the null hypothesis. Overall, the significance of the model increases as the f-value increases or the p-value decreases [74,75].

For the effective torque response parameter, the R^2 value is 0.9624 and the Adj. R^2 value is 0.881. The high R^2 value and the difference between the Adj. R^2 value and<0.2 increased the reliability and accuracy. The model created for estimating the effective torque value depending on different input parameters is given in Equation (9).

$$T_{eff}\ (Nm) = 5.17 + 1.08A - 0.075B - 0.275C + 0.1444AB - 0.2556AC - 0.0556BC - 0.1278A^2 + 0.1222B^2 - 0.1778C^2 - 0.1069ABC - 0.03188A^2B + 0.0681A^2C - 0.4319AB^2 \tag{9}$$

3. Results and discussion

The results obtained for different response parameters were examined in detail. ANOVA results are included, and the F-value and p-value values are examined and the importance of variable input parameters on output parameters is mentioned. In addition, it is necessary to apply various test methods in order to verify the models created [56]. If the P-value is<0.05, it means that the variable parameter is important, and if it is greater than 0.05, it means that it is insignificant [57,58]. The magnitude of the F-value indicates the magnitude of the effect of that variable parameter on the response parameter.

R^2 and Adj. R^2 values are examined in order to evaluate the accuracy of statistical results generated by RSM [59]. The magnitude of the R^2 value is seen as an indicator of the similarity between the statistical

The effective torque produced in the engine may vary with the input parameters, the fuel used and the fuel additives used [61]. The change in the effective torque value depending on the naphtha ratio, engine speed and lambda value is shown in Fig. 3. It was observed that the increase in the naphtha ratio caused an increase in the effective torque value. The fact that the octane number of naphtha fuel is higher than that of *n*-heptane fuel shifted the CA10 and CA50 values and brought them to optimum points [62]. This resulted in an increase in the effective torque. It has been observed that the effective torque is low when the engine speed is between 1200 and 1300 rpm. As the engine speed rises above a certain level, a slight decrease is observed with the expansion of the cylinder volume, since the heat release rate and the maximum in-cylinder pressure value are revealed after TDC. The increase in lambda value caused a decrease in the effective torque value in the use of

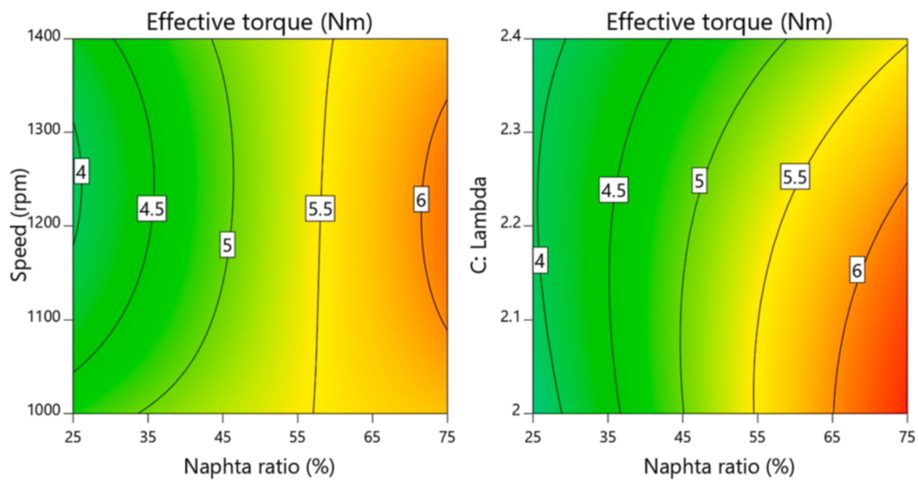

Fig. 3. Effect of engine input parameters on effective torque.

Table 7
ANOVA results for indicated thermal efficiency.

Source	Sum of Squares	Mean Square	F-value	p-value	Remarks
Model	589.91	45.38	1409.92	< 0.0001	significant
A-Naphtha ratio	203.87	203.87	6334.56	< 0.0001	significant
B-Engine speed	17.66	17.66	548.63	< 0.0001	significant
C-Lambda	72.51	72.51	2253.03	< 0.0001	significant
Residual	0.1931	0.0322			
Cor Total	590.1				

Table 8
ANOVA results for BSFC.

Source	Sum of Squares	Mean Square	F-value	p-value	Remarks
Model	86594.9	6661.15	5	0.0292	significant
A-Naphtha ratio	54896.41	54896.41	41.21	0.0007	significant
B-Engine speed	389.76	389.76	0.2926	0.6080	Not significant
C-Lambda	40.77	40.77	0.0306	0.8669	Not significant
Residual	7992.13	1332.02			
Cor Total	94587.03				

naphtha in the fuel mixture content above 40 %. The highest effective torque value was determined as 6.6 Nm when the naphtha ratio was 75 %, the lambda was 2 and the engine speed was 1200 rpm.

3.1.2. *Indicated thermal efficiency*

ANOVA results for the indicated thermal efficiency are given in Table 7. It was determined that the naphtha ratio, engine speed and lambda values were important for the indicated thermal efficiency value. While the highest F-value value is obtained with the naphtha ratio, it is seen that this value is followed by lambda and engine speed.

The R2 value for the ITE response parameter is 0.9997 and the Adj. R2 value is 0.999. The fact that the R2 value is high and the difference between the Adj. R2 value is less than 0.2 strengthened the accuracy of the results obtained for the ITE. The model created for estimating the indicated thermal efficiency value depending on different input parameters is given in Equation (10).

$$\begin{aligned} ITE\ (\%) = {} & 29.12 + 5.0482A + 1.4856B + 3.0106C - 0.3501AB - 1.9493AC - 1.8077BC - 0.8631A^2 \\ & + 0.56307B^2 - 0.1357C^2 - 0.031ABC - 2.8823A^2B - 0.2181A^2C - 1.0689AB^2 \end{aligned} \tag{10}$$

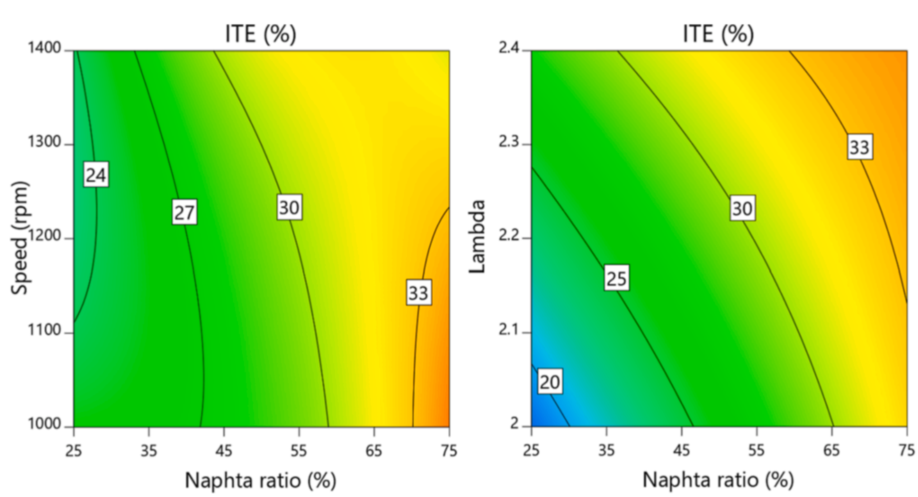

Fig. 4. Effect of engine input parameters on ITE value.

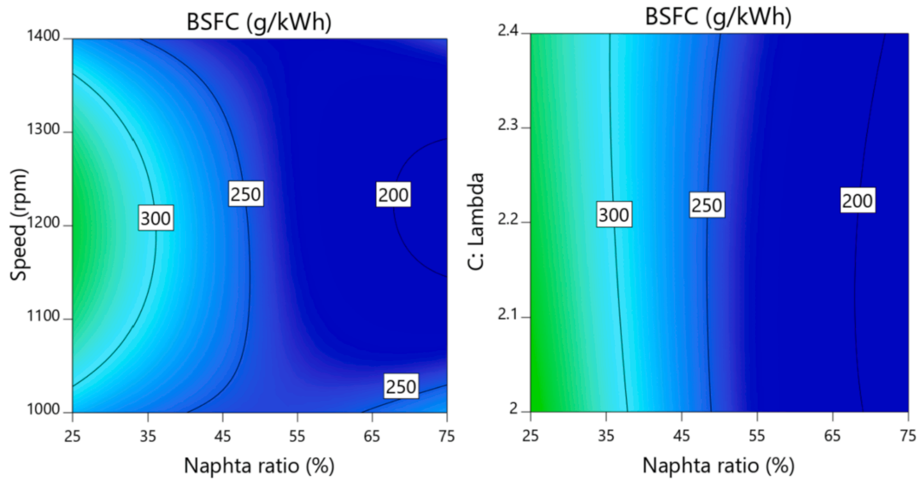

Fig. 5. Effect of engine input parameters on BSFC value.

Table 9
ANOVA results for CA10.

Source	Sum of Squares	Mean Square	F-value	p-value	Remarks
Model	335.22	25.79	71.84	< 0.0001	significant
A-Naphtha ratio	149.3	149.3	415.98	< 0.0001	significant
B-Engine speed	37.32	37.32	103.99	< 0.0001	significant
C-Lambda	5.38	5.38	14.99	0.0083	significant
Residual	2.15	0.3589			
Cor Total	337.37				

The variation of indicated thermal efficiency value depending on naphtha ratio, lambda value and engine speed is shown in Fig. 4. The increase in the naphtha ratio caused an increase in the ITE value. As the naphtha ratio increased, the octane number of the blended fuel increased. The increase in the octane number delayed the ignition start of the filler in the cylinder. In addition, the optimum ignition onset time was achieved and an efficient shot was achieved. It was observed that the ITE value increased with the increase of the engine speed. The increase in engine speed ensures that the fuel-air mixture is more homogeneous and the combustion takes place with a higher quality. This is thought to be the reason for the increase in yield. With the increase in lambda value, significant increases in ITE value were observed. The decrease in MPRR with an increase in the naphtha ratio also increases the ITE value [63]. With the depletion of the mixture, all of the fuel sent into the cylinder meets with oxygen and all fuel is burned. This causes an increase in the ITE value. The highest ITE value was determined as 37.21% at 75% naphtha ratio, 2.4 lambda ratio and 1000 rpm engine speed.

3.1.3. Brake spesific fuel consumption (BSFC) (g/kWh)

ANOVA results for BSFC are given in Table 8. It was determined that the BSFC value was significant for the naphtha ratio and insignificant for the engine speed and lambda values. The highest F-value was obtained with the naphtha ratio.

The R^2 value for the BSFC response parameter is 0.9155 and the Adj. R^2 value is 0.7324. The difference between the R^2 value and the Adj. R^2 value was<0.2, which strengthened the accuracy of the results obtained

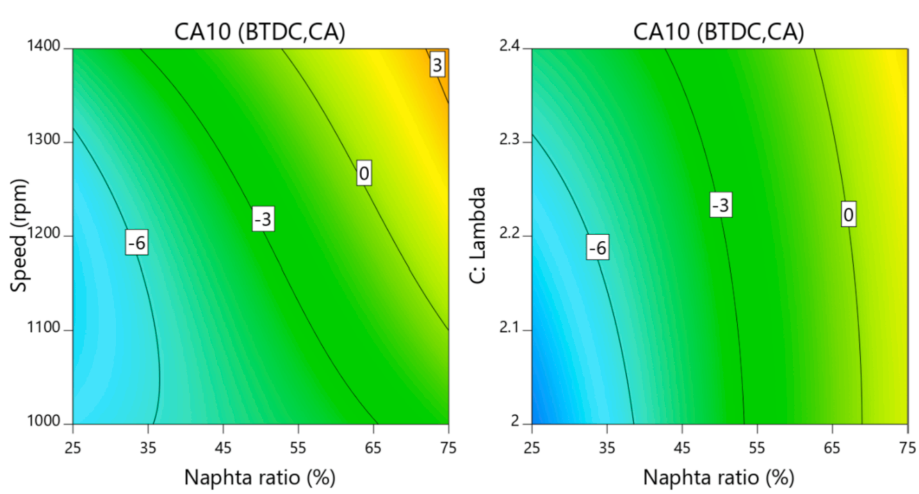

Fig. 6. Effect of engine input parameters on CA10 value.

for BSFC. The model created for estimating the BSFC value depending on different input parameters is given in Equation (11).

$$BSFC\,(g/kWh) = 244.46 - 82.8375A - 6.98B + 2.2575C - 4.45875AB + 8.50375AC - 1.1487BC + 30.0056A^2 - 8.07069B^2 + 3.67306C^2 + 8.42875ABC - 1.22625A^2B - 10.7463A^2C + 73.7738AB^2 \tag{11}$$

Studies are carried out on the improvement of the BSFC value by using different methods on the internal combustion engine. The change in the BSFC value depending on the naphtha ratio, engine speed and lambda value is shown in Fig. 5. It is observed that the BSFC value increased with the decrease in the naphtha ratio. If the engine speed is about 1200 rpm, an increase in the BSFC value is observed. The reason for this is the decrease in engine torque value and in parallel engine power at 1200 rpm. The calorific value of naphtha fuel is lower than that of *n*-heptane. In this case, an increase in BSFC value is expected with an increase in the naphtha ratio in the fuel mixture [37]. However, the increase in the naphtha ratio delays the ignition time and increases the ITE values. However, an improvement is observed in BSFC consumption. Özer and Vural investigated the effect of CNG addition in a diesel engine fueled by diesel/*n*-heptane and diesel/toluene. With the addition of toluene to diesel fuel, there is an increase in fuel consumption values at all engine loads compared to diesel fuel, and a decrease with the addition of *n*-heptane. It was seen that the high calorific value and cetane number of nheptan added to the diesel fuel partially affected the combustion positively, and with the improvement of combustion[76]. The highest BSFC value was determined as 350 g/kWh when the naphtha ratio was 25 %, the lambda was 2, and the engine speed was 1200 rpm.

3.1.4. cA10

The CA10 value defines the CA (crankshaft angle) at which 10 % of the combustion time is completed [64]. ANOVA results for CA10 are given in Table 9. It was determined that the naphtha ratio, engine speed and lambda values were important for the CA10 value. The highest F-value is naphtha ratio, engine speed and lambda value, from high to low, respectively.

The R^2 value for the CA10 response parameter is 0.9936 and the Adj. R^2 value is 0.9798. The difference between the R^2 value and the Adj. R^2 value was<0.2, which strengthened the accuracy of the results obtained for CA10. The model created for estimating the CA10 value depending on different input parameters is given in Equation (12).

$$CA10\,(o\,CA) = -3.11 + 4.32A + 2.16B + 0.82C + 0.7425AB - 0.6975AC - 0.4275BC + 0.243864A^2 + 0.513864B^2 + 0.283864C^2 + 0.3375ABC - 0.2925A^2B + 0.5075A^2C - 1.1025AB^2 \tag{12}$$

The CA10 value is accepted as the start of combustion in many studies. The variation of CA10 value depending on naphtha ratio, engine speed and lambda value is given in Fig. 6. It is seen that the CA10 value is delayed depending on the naphtha ratio. The reason for this is that with the increase in the naphtha ratio, the octane number increases and ignition becomes more difficult [65]. In the HCCI engine, ignition takes place by itself. In this case, ignition onset is more affected by fuel properties. As the engine speed increases, the homogeneity of the filler mixture improves and faster combustion is expected. However, in the results obtained within the scope of this study, it is seen that the CA10 value is delayed with the increase in engine speed. This is because the time required for ignition passes faster at higher engine speeds. As a result of a faster pass, reaching the required temperature for auto-ignition occurs in the process of turning more crankshaft angle [28]. An increase in CA10 value was observed with the increase of lambda. This is because as lambda increases, the mixture becomes poorer and ignition becomes more difficult. The highest CA10 value was determined as a crankshaft angle of 4 when the naphtha ratio was 75 %, the lambda ratio was 2.4, and the engine speed was 1400 rpm.

3.1.5. cA50

The CA50 value defines the CA at which 50 % of the combustion time is completed [66]. ANOVA results for CA50 are given in Table 10. It was determined that the naphtha ratio, engine speed and lambda values were important for the CA50 value. The highest F-value is naphtha ratio, engine speed and lambda, from high to low, respectively.

The R^2 value for the CA50 response parameter is 0.9993 and the Adj. R^2 value is 0.9978. The difference between the R^2 value and the Adj. R^2 value was<0.2, which strengthened the accuracy of the results obtained for CA50. The model created for estimating the CA50 value depending on different input parameters is given in Equation (13).

$$CA50\,(o\,CA) = 1.4943 + 5.4A + 2.61B + 1.2375C + 1.075AB - 0.545AC - 0.545BC + 0.117159A^2 + 0.252159B^2 + 0.308409C^2 + 0.725ABC + 0.275A^2B + 1.1075A^2C - 1.435AB^2 \tag{13}$$

The CA50 value is aimed to occur when the piston crosses the top dead center by 7–11 °CA [65]. The variation of CA50 value depending on the naphtha ratio, engine speed and lambda value is shown in Fig. 7. As the naphtha ratio increases, the octane number of the blended fuel increases. With the increase in the octane number, combustion becomes more difficult and an increase in the CA50 value is observed. It is seen that the CA50 value approaches the top dead point and is delayed with the increase in lambda and engine speed parameters. The reason for this is that the combustion takes place more controlled with the increase in the lambda value. Shifting the CA50 value from the top dead center provides a high positive contribution to engine performance and efficiency. The highest CA50 value was determined as 11.8 crankshaft angle when the naphtha ratio was 75 %, the lambda ratio was 2.4, and the engine speed was 1400 rpm.

3.1.6. Combustion duration

ANOVA results for CD are given in Table 11. It was determined that the naphtha ratio, engine speed and lambda values were important for the CD value. The highest F-value values, from high to low, are engine speed, lambda and naphtha ratio, respectively.

The R^2 value for the CD response parameter is 0.9974 and the Adj. R^2 value is 0.9918. The fact that the R^2 value was high and the difference between the Adj. R^2 value was<0.2 strengthened the accuracy of the results obtained for CD. The model created for estimating the Combustion duration value depending on different input parameters is given in Equation (14).

$$CD\ (o\,CA) = 29.17 - 0.45A - 1.035B + 0.7075C + 0.585AB + 0.585AC + 0.405BC + 0.6492A^2 + 0.4017B^2 \\ -0.0195C^2 - 0.045ABC + 0.81A^2B - 0.2125A^2C - 0.855AB^2 \tag{14}$$

Cobustion duration (DC) defines the crankshaft angle value between the start and end of the combustion process. The change in CD value depending on the naphtha ratio, engine speed and lambda value is shown in Fig. 8. It was observed that the combustion time value decreased with the increase of engine speed and lambda parameters. The increase in the lambda value causes a decrease in the combustion end temperature and provides a more controlled combustion process. This causes an increase in the burning time. With the increase of the naphtha ratio, the combustion time was expected to increase, but a decrease was observed. The reason for this is thought to be xxxx. The highest combustion duration value was determined as a crankshaft angle of 33 when the knuckle ratio was 25%, the lambda was 2, and the engine speed was 1000 rpm.

3.1.7. Cov_{imep}

COV_{imep} are used to determine the differences that occur in internal combustion engine cycles. ANOVA results for COV_{imep} are given in Table 12. It was determined that the naphtha ratio and lambda values were significant for the COV_{imep} value, and the engine speed value was insignificant. The highest F-value is lambda, naphtha ratio and engine speed, from high to low, respectively.

The R^2 value for the COV_{imep} response parameter is 0.9966 and the Adj. R^2 value is 0.9893. The fact that the R^2 value was high and the difference between the Adj. R^2 value was<0.2 strengthened the accuracy of the results obtained for COV_{imep}. The model created for estimating the COV_{imep} value depending on different input parameters is given in Equation (15).

$$COVimep = 1.49 - 1.07A - 0.215B - 1.71C + 0.8037AB + 0.8462AC + 0.6137BC + 0.497614A^2 \\ +0.1001B^2 + 1.1926C^2 - 0.7187ABC - 0.2737A^2B + 0.0537A^2C + 0.2187AB^2 \tag{15}$$

The variation of the COV_{imep} value depending on the naphtha ratio, engine speed and lambda value is shown in Fig. 9. A decrease in COV_{imep} value is observed depending on the increase in engine speed and lambda. Increasing engine speed improves fuel–air mixture. The homogeneous mixture ensures more stable operation of the engine and minimizes the differences between the cycles. It is deduced that the combustion takes place in a more controlled manner with the increase in lambda and naphtha ratios. Controlled combustion ensures that the cycles are maintained more stable and leads to an improvement in the COV_{imep} value. The highest COV_{imep} value was determined as 25 % in the case of naphtha rate, 2 lambda and 9 % at the engine speed of 1000 rpm.

3.1.8. MPRR (bar/CA)

The MPRR is used to estimate the knocking tendency of the engine [67]. ANOVA results for MPRR are given in Table 13. It was determined that the naphtha ratio, lambda values were significant and the engine speed value was insignificant for the MPRR value. The highest F-value is lambda, naphtha ratio and engine speed, from high to low, respectively.

The R^2 value for the MPRR response parameter is 0.9939 and the Adj. R^2 value is 0.9805. The fact that the R^2 value was high and the difference between the Adj. R^2 value was<0.2 strengthened the accuracy of the results obtained for i MPRR. The model created for estimating the MPRR value depending on different input parameters is given in Equation (16).

$$MPRR = 7.13 - 1.8805A - 0.0787B - 2.6844C + 0.6476AB + 0.6107AC + 0.2939BC - 0.0632A^2 \\ +0.0685B^2 + 0.6041C^2 - 0.9490ABC - 0.4362A^2B - 0.1513A^2C + 0.9118AB^2 \tag{16}$$

An increase was observed in the MPRR value depending on the increase in engine speed, lambda and naphtha ratios. The change in MPRR value depending on the naphtha ratio, engine speed and lambda value is shown in Fig. 10. In cases where the lambda is low, there is an increase in the amount of fuel taken into the cylinder. As more fuel is burned at small crankshaft angles, high amounts of heat occur suddenly. Sudden increases in the amount of heat also cause sudden pressure increases [68]. As a result, sudden increases are experienced in the MPRR value. It is not appropriate to reduce the lambda value below a certain level, as HCCI will prevent the engine from running due to loud noise and vibrations. With the increase in the naphtha ratio, the MPRR value also decreases because the fuel becomes more difficult to burn. In addition, the octane number, which increases with the naphtha ratio, also improves its resistance to knocking. The highest MPRR value was determined as 14.83 bar/CA when the naphtha ratio was 25 %, the lambda was 2, and the engine speed was 1000 rpm.

3.2. Examination of emission response parameters

One of the most important problems in internal combustion engines is the realization of emissions. The most important emissions in internal combustion engines are UHC, NOx, CO and particulates. High homogeneity is achieved in HCCI combustion mode and NOx and particle emissions are significantly reduced [69,70]. In this study, the measurement of NOx emissions was carried out, but because it was at very low values, it was neglected and was not included in the study.

3.2.1. Unburned hydrocarbon emissions (UHC)

UHC is a type of emission that occurs due to the main reasons of excess fuel, lack of oxygen and low end-of-combustion temperatures in the internal combustion engine [71]. ANOVA results for UHC are given in Table 14. For the UHC value, it was determined that the naphtha ratio, lambda values were significant and the engine speed value was insignificant. The highest F-value is lambda, naphtha ratio and engine speed, from high to low, respectively.

The R^2 value for the UHC response parameter was determined as 0.9523 and the Adj. R^2 value was determined as 0.849. The fact that the R^2 value was high and the difference between the Adj. R^2 value was<0.2 strengthened the accuracy of the results obtained for UHC. The model created for estimating the UHC value depending on different input parameters is given in Equation (17).

Table 10
ANOVA results for CA50.

Source	Sum of Squares	Mean Square	F-value	p-value	Remarks
Model	557.89	42.91	661.14	< 0.0001	significant
A-Naphtha ratio	233.28	223.28	3593.89	< 0.0001	significant
B-Engine speed	54.5	54.5	839.57	< 0.0001	significant
C-Lambda	12.25	12.25	188.74	< 0.0001	significant
Residual	0.3895	0.0649			
Cor Total	558.28				

$$UHC = 421.77 - 69.25A - 19B - 71.25C - 4.25AB + 20AC + 12.75BC + 14.2614A^2 \\ -5.3636B^2 + 21.5114C^2 - 8.75ABC + 24.25A^2B + 40.75A^2C + 13.25AB^2 \qquad (17)$$

The variation of the UHC value depending on the naphtha ratio, engine speed and lambda value is shown in Fig. 11. A decrease was observed in HC emission, depending on naphtha, lambda value and engine speed. Poorer mixtures are expected to increase UHC and CO emissions, as they reduce heat dissipation and the temperatures of combustion gases. However, with the decrease of lambda, oxygen deficiency starts in the cylinder. Accordingly, an increase in HC emission is observed. An increase in engine torque was observed with an increase in the naphtha ratio. The observed increase in engine torque also increases the in-cylinder combustion end temperature. In this context, the increase in the naphtha ratio causes the UHC emission to improve [72]. Moreover, Özer and Vural observed the addition of *n*-heptane to diesel fuel decreased HC emissions at all engine loads[76]. The highest UHC value was determined as 578.73 ppm when the naphtha ratio was 25 %, lambda 2 was and the engine speed was 1150 rpm.

3.2.2. Carbon monoxide (CO)

In the combustion process, CO emission occurs due to lack of oxygen, inhomogeneous mixture and low end-of-combustion temperature [73]. ANOVA results for CO emissions are given in Table 15. It was determined that the naphtha ratio, lambda values were significant for the CO value, and the engine speed value was insignificant. The highest F-value values are naphtha ratio, lambda and engine speed, from high to low, respectively.

The R^2 value for the CO response parameter is 0.9186 and the Adj. R^2 value is 0.7423. The fact that the difference between the R^2 value and the Adj. R^2 value was<0.2 strengthened the accuracy of the results obtained for CO. The model created for estimating the CO value depending on different input parameters is given in Equation (18).

$$CO = 0.08 - 0.0297\,A + 0.0075\,B + 0.0237C - 0.0011AB - 0.00015AC + 0.0069BC + 0.0083A^2 \\ +0.0004B2 + 0.0043C^2 + 0.0005ABC + 0.0049A^2B - 0.0048A^2C + 0.015025AB^2 \qquad (18)$$

The variation of the CO value depending on the naphtha ratio, engine speed and lambda value is shown in Fig. 12. With the increase in naphtha ratio and decrease in lambda, improvement in CO emission is observed. With the increase in lambda, it is expected that the amount of oxygen will increase and the amount of CO will decrease accordingly. However, the reason for the increase in the amount of CO is estimated to be the decrease in the combustion end temperature. The reason for the decrease in the CO emission with the increase of the naphtha ratio is the increase in the combustion end temperature with the increase in the effective torque. No stable increase or decrease in CO emission change was observed depending on the change in engine speed. The highest CO value was determined as 25 % in the naphtha ratio, 2.4 % lambda and 0.147 % in the engine speed at 1350 rpm.

3.3. Comparison of experimental and statistical data

The graphs comparing the accuracy of the experimental and RSM response parameter results are given in Fig. 13. As can be seen in the figure, the estimated and actual values of all response parameters are very close to the fit line. The closeness of these parameters to the fit line means that the estimated values are very close to the actual values and have high accuracy.

3.4. Optimization

RSM optimization was performed using input and response parameters. Naphtha ratio, engine speed and effective torque are taken as input parameters. Effective torque, Indicated thermal efficiency, BSFC, CA50, COV_{imep}, MPRR, UHC and CO values are taken as output parameters. Approach, lower and upper limit values of input and response parameters and optimized parameter value are given in Table 16. During the optimization process, the lower and upper limits of the parameters were determined by RSM. In the approach part, the minimum, maximum or value range targeted in the response parameters is entered. It is aimed to maximize the effective torque and thermal efficiency on an HCCI engine, and to minimize BSFC, UHC and CO emissions. In range approach was chosen for CA50, COV_{imep} and MPRR values and acceptable limit values were determined as 7–11 °CA, 1–6 % and 1–8 bar/°CA, respectively. Since there is no target value for CA10 and combustion duration values, they are not included in the optimization.

The desirability rate, which is a parameter of the accuracy of the optimization, was determined as 0.925. The fact that the desirability rate value is close to 1 strengthens the suitability of the optimization made. After the optimization, the optimum input parameter values were determined as 75 % naphtha ratio, 1166.75 rpm engine speed and 2.12 lambda value. Depending on the optimum input parameters, the

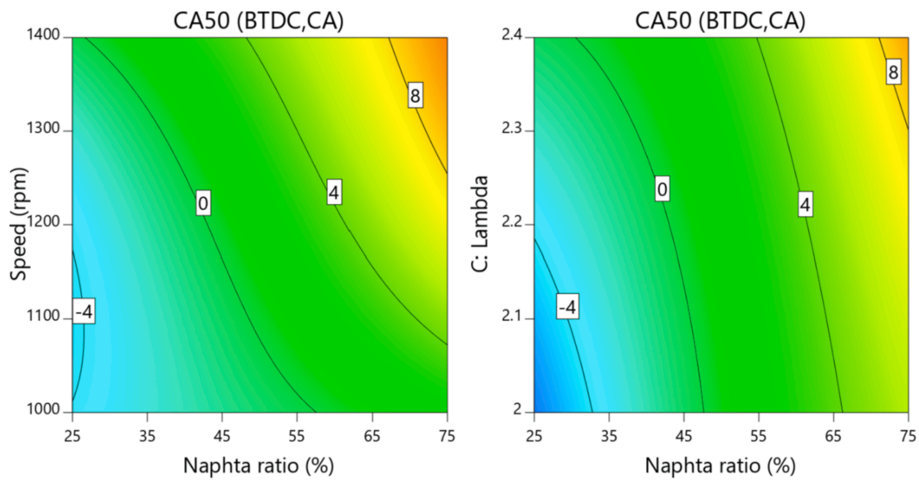

Fig. 7. Effect of engine input parameters on CA50 value.

Table 11
ANOVA results for combustion duration.

Source	Sum of Squares	Mean Square	F-value	p-value	Remarks
Model	50.54	3.89	177.09	< 0.0001	significant
A-Naphtha ratio	1.62	1.62	73.79	< 0.0001	significant
B-Engine speed	8.57	8.57	390.32	< 0.0001	significant
C-Lambda	4.00	4.00	182.39	< 0.0001	significant
Residual	0.1317	0.0220			
Cor Total	50.68				

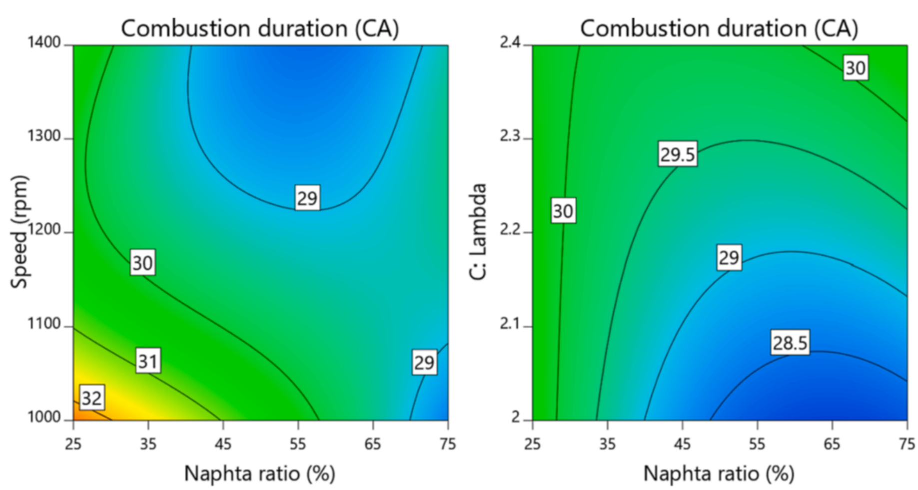

Fig. 8. Effect of engine input parameters on CD value.

Table 12
ANOVA results for $COV_{imep.}$

Source	Sum of Squares	Mean Square	F-value	p-value	Remarks
Model	118.99	9.15	136.41	< 0.0001	significant
A-Naphtha ratio	9.16	9.16	136.50	< 0.0001	significant
B-Engine speed	0.3698	0.3698	5.51	0.0572	Not significant
C-Lambda	23.39	23.39	348.62	< 0.0001	significant
Residual	0.4026	0.0671			
Cor Total	119.39				

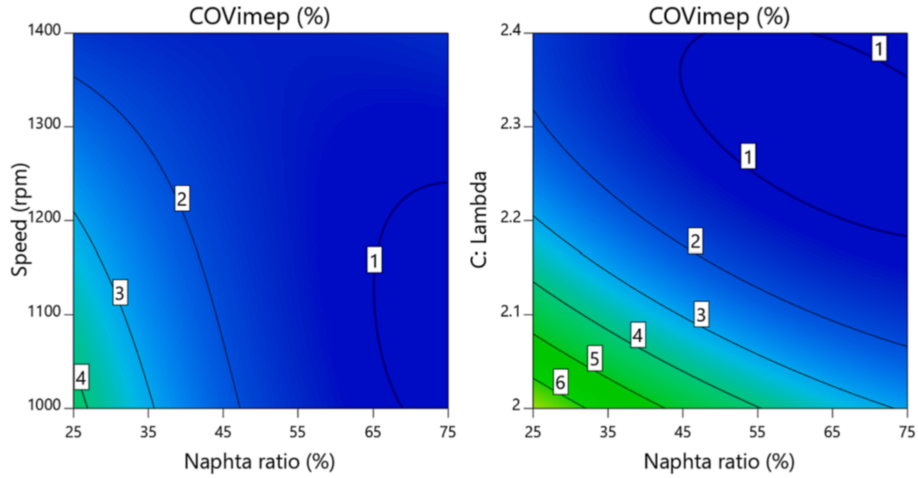

Fig. 9. Effect of engine input parameters on COV imep value.

Table 13
ANOVA results for MPRR.

Source	Sum of Squares	Mean Square	F-value	p-value	Remarks
Model	184.37	14.18	74.68	< 0.0001	significant
A-Naphtha ratio	28.29	28.29	148.98	< 0.0001	significant
B-Engine speed	0.0496	0.0496	0.2612	0.6276	Not significant
C-Lambda	57.65	57.65	303.59	< 0.0001	significant
Residual	1.14	1.14			
Cor Total	185.51				

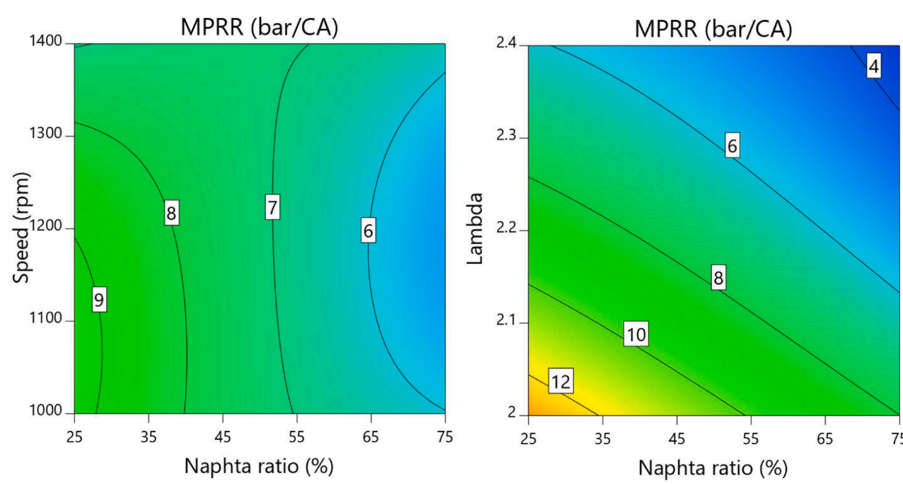

Fig. 10. Effect of engine input parameters on MPRR value.

Table 14
ANOVA results for UHC.

Source	Sum of Squares	Mean Square	F-value	p-value	Remarks
Model	1.377E + 5	10590.08	9.22	0.0061	significant
A-Naphtha ratio	38364.5	38364.5	33.39	0.0012	significant
B-Engine speed	2888.0	2888.0	2.51	0.164	Not significant
C-Lambda	40612.5	40612.5	35.34	0.001	significant
Residual	6894.82	1149.14			
Cor Total	1.446E + 05				

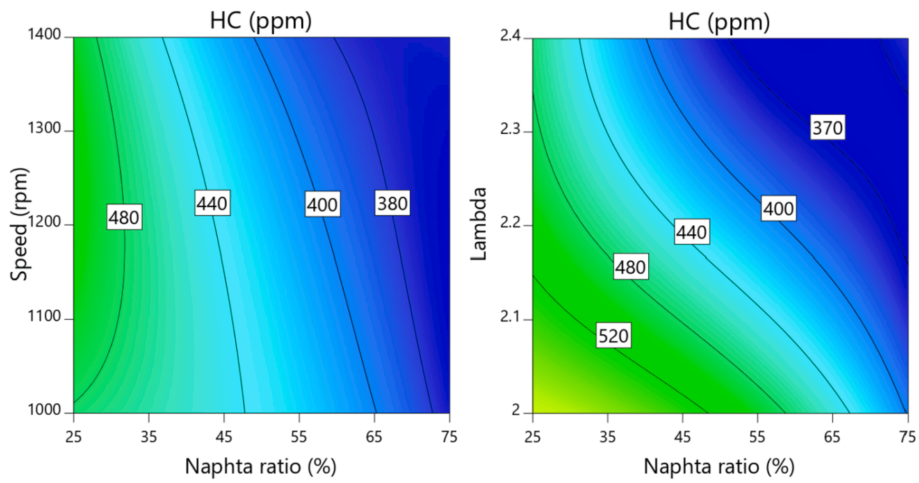

Fig. 11. Effect of engine input parameters on UHC value.

Table 15
ANOVA results for CO.

Source	Sum of Squares	Mean Square	F-value	p-value	Remarks
Model	0.0202	0.0016	5.21	0.0264	significant
A-Naphtha ratio	0.0071	0.0071	23.68	0.0028	significant
B-Engine speed	0.0004	0.0004	1.51	0.2658	Not significant
C-Lambda	0.0045	0.0045	15.09	0.0081	significant
Residual	0.0018	0.0018			
Cor Total	0.022				

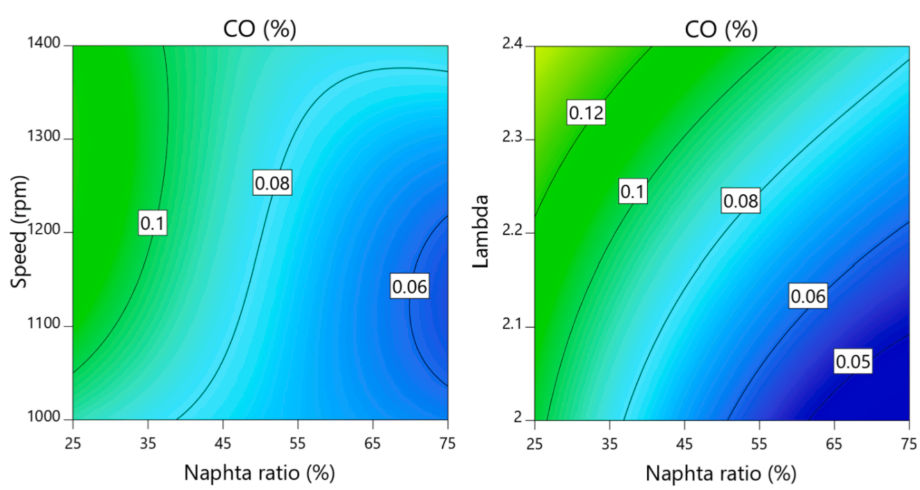

Fig. 12. Effect of engine input parameters on CO value.

effective torque value of 6.26 Nm and ITE 33.09 % were found to be very close to the targeted maximum values. It has been determined that the optimized HC value is 375.96 ppm and the CO value is 0.05 %, and the result is very close to the targeted minimum values.

4. Conclusion

In this study, the effects of HCCI engine input parameters and the use of different fuels on combustion, performance and emissions were investigated experimentally and statistically. The engine speed was determined as 800–1600 rpm, the lambda value was 1.8–2.6 and the naphtha ratio in the mixed fuel was 0–100 %. As a result of the study, ANOVA tables, model equations, contour graphs of effective torque, indicated thermal efficiency, BSFC, CA10, CA50, Combustion duration, COV_{imep}, MPRR, UHC and CO response parameters were created and the effect of input parameters was examined in detail.

With the increase in the naphtha ratio, an increase in the effective torque, ITE, was observed. The main reason for this situation is seen as the increase in the octane number of the blended fuel as the naphtha ratio increases and the reduction of the CA10 value to the targeted values with the formation of resistance against ignition. It was observed that the BSFC value did not change much with the lambda value, but there was a serious improvement with the increase in the naphtha ratio. Although an increase was observed in CA10 and CA50 values depending on the increase in lambda value and engine speed, no stable increase or decrease was observed in the combustion duration value. With the increase in engine speed, lambda and naphtha ratio, improvement in COV_{imep} and MPRR values was observed and it was determined that the

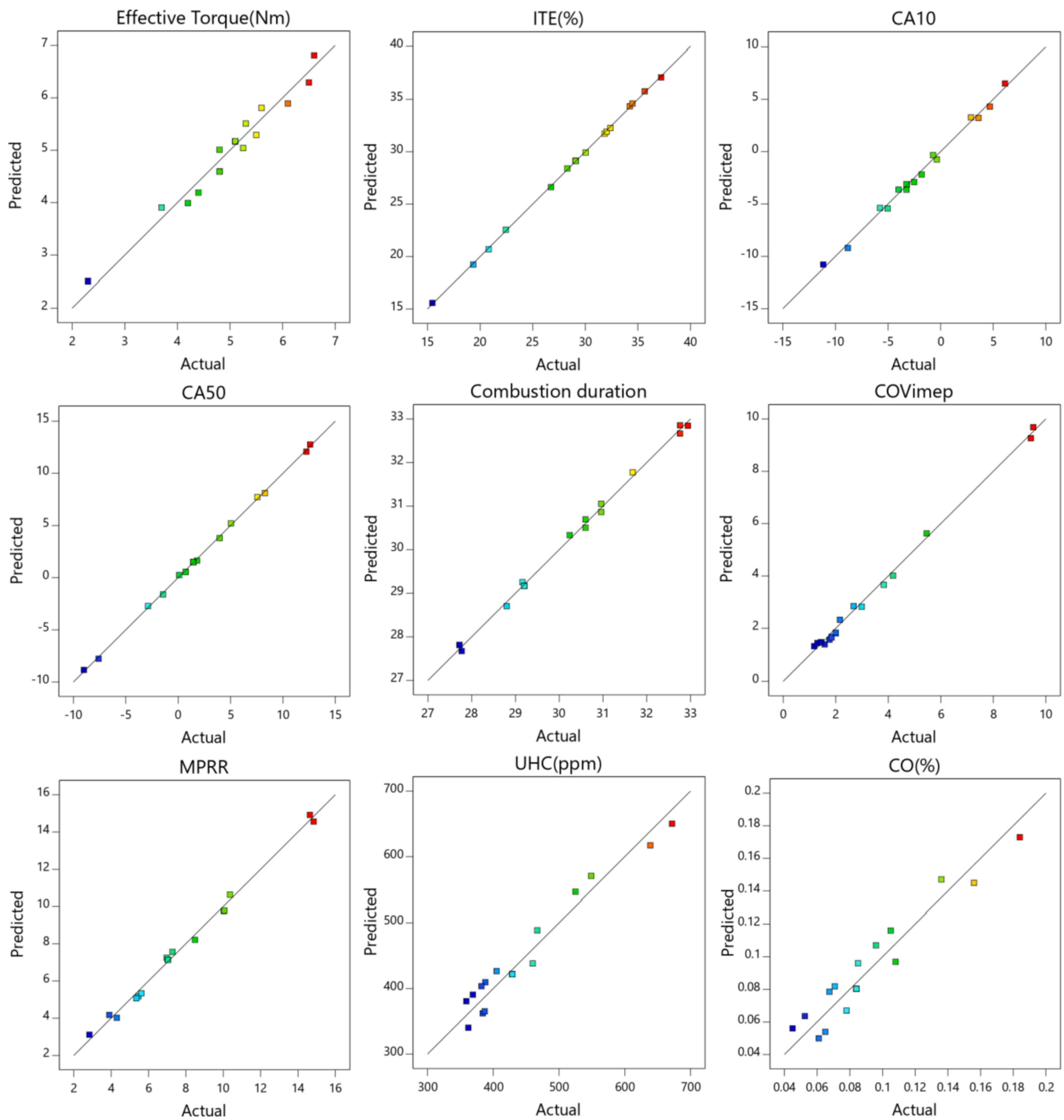

Fig. 13. Comparison of experimental and RSM response parameters.

Table 16
Criterias and results of optimization.

Parameter	Target	Limits Lower	Upper	Optimized input and response parameters	Unit
A-Naphtha ratio (%)	In range	25	75	75	%
B-Engine speed	In range	1000	1400	1166.75	rpm
C-Lambda	In range	2	2.4	2.12	–
Effective torque	Maximize	2.3	6.6	6.26	Nm
Indicated thermal efficiency	Maximize	15.45	37.21	33.09	%
BSFC	Minimize	217.7	553.5	196.79	g/kWh
CA10	None	−11.16	6.12	0.77	°CA
CA50	In range (7–11)	−9	12.6	5.6	°CA
Combustion duration	None	27.72	32.94	28.84	°CA
COV_{imep}	In range (1–6)	1.18	9.52	1.46	%
MPRR	In range (1–8)	2.83	14.84	6.24	Bar/°CA
HC	Minimize	359	672	375.96	ppm
CO	Minimize	0.045	0.184	0.05	%

engine worked more stable. It was determined that the value of UHC emission decreased with the increase of variable parameter values. On the other hand, while there was a decrease in the CO emission values due to the increase in the naphtha ratio, an increase was observed due to the increase in the lambda value.

After the optimization, the desirability rate, which is a parameter of the accuracy of the optimization, was determined as 0.925. The optimum input parameters were calculated as 75 % naphtha ratio, 1166.75 rpm engine speed and 2.12 lambda value. The response parameter values obtained depending on the optimum input parameters are effective torque 6.26 Nm, indicated thermal efficiency 33.09 %, BSFC 196.79 g/kWh, CA10 0.77 °CA, CA50 5.6 °CA, combustion duration 28.84 °CA, COV_{imep} 1.46 %, MPRR It was determined as 6.24 bar/°CA, HC 375.96 ppm and CO 0.05 %.

CRediT authorship contribution statement

Tolga Kocakulak: Methodology, Writing – original draft, Investigation, Writing – review & editing. **Serdar Halis:** Methodology, Writing – original draft, Investigation. **Seyed Mohammad Safieddin Ardebili:** Supervision, Writing – review & editing. **Mustafa Babagiray:** Methodology, Investigation, Writing – review & editing. **Can Haşimoğlu:** Supervision, Project administration. **Masoud Rabeti:** Writing – review & editing. **Alper Calam:** Methodology, Investigation, Writing – review & editing.

Declaration of Competing Interest

The authors declare that they have no known competing financial interests or personal relationships that could have appeared to influence the work reported in this paper.

Data availability

No data was used for the research described in the article.

References

[1] Calam, T. T. (2021). Electrochemical Behavior and Voltammetric Determination of 2-Nitrophenol on Glassy Carbon Electrode Surface Modified with 1-Amino-2-Naphthol-4-Sulphonic Acid. Eng Perspect, 1(1), 1-5. https://doi.org/10.29228/sciperspective.48525.

[2] Tabanlıgil Calam T, Yılmaz EB. Electrochemical determination of 8-hydroxyquinoline in a cosmetic product on a glassy carbon electrode modified with 1-amino-2-naphthol-4-sulphonic acid. Instrum Sci Technol 2021;49(1):1–20.

[3] Tabanlıgil Calam T. Analytical application of the poly (1H–1, 2, 4-triazole-3-thiol) modified gold electrode for high-sensitive voltammetric determination of catechol in tap and lake water samples. Int J Environ Anal Chem 2019;99(13):1298–312.

[4] Calam TT. Electrochemical Oxidative Determination and Electrochemical Behavior of 4-Nitrophenol Based on an Au Electrode Modified with Electro-polymerized 3, 5-Diamino-1, 2, 4-triazole Film. Electroanalysis 2020;32(1):149–58.

[5] Lion, S., Vlaskos, I., & Taccani, R. (2020). A review of emissions reduction technologies for low and medium speed marine Diesel engines and their potential for waste heat recovery. Energy Conversion and Management, 207, 112553.

[6] Abed KA, Gad MS, El Morsi AK, Sayed MM, Elyazeed SA. Effect of biodiesel fuels on diesel engine emissions. Egypt J Pet 2019;28(2):183–8.

[7] Alrazen HA, Ahmad KA. HCNG fueled spark-ignition (SI) engine with its effects on performance and emissions. Renew Sustain Energy Rev 2018;82:324–42.

[8] Lawler B, Lacey J, Güralp O, Najt P, Filipi Z. HCCI combustion with an actively controlled glow plug: The effects on heat release, thermal stratification, efficiency, and emissions. Appl Energy 2018;211:809–19.

[9] Gainey, B., O'Donnell, P., Yan, Z., Moser, S., & Lawler, B. (2021). LTC performance of C1–C4 water-alcohol blends with the same cooling potential. Fuel, 293, 120480.

[10] Kocakulak T, Solmaz H. Control of pre and post transmission parallel hybrid vehicles with fuzzy logic method an comparison with other power systems. Journal of the Faculty of Engineering and Architecture of Gazi University 2020;35(4).

[11] Pelletier S, Jabali O, Laporte G, Veneroni M. Battery degradation and behaviour for electric vehicles: Review and numerical analyses of several models. Transportation Research Part B: Methodological 2017;103:158–87.

[12] Dudley, B. (2018). BP statistical review of world energy. BP Statistical Review, London, UK, accessed Aug, 6(2018), 00116.

[13] Yılmaz E, Solmaz H, Polat S, Altin M. Effect of the three-phase diesel emulsion fuels on engine performance and exhaust emissions. Journal of the Faculty of Engineering and Architecture of Gazi University 2013;28(1):127–34.

[14] Calam, A., Aydoğan, B., & Halis, S. (2020). The comparison of combustion, engine performance and emission characteristics of ethanol, methanol, fusel oil, butanol, isopropanol and naphtha with n-heptane blends on HCCI engine. Fuel, 266, 117071.

[15] Shim, E., Park, H., & Bae, C. (2020). Comparisons of advanced combustion technologies (HCCI, PCCI, and dual-fuel PCCI) on engine performance and emission characteristics in a heavy-duty diesel engine. Fuel, 262, 116436.

[16] Duan, X., Lai, M. C., Jansons, M., Guo, G., & Liu, J. (2021). A review of controlling strategies of the ignition timing and combustion phase in homogeneous charge compression ignition (HCCI) engine. Fuel, 285, 119142.

[17] Bahrami, S., Poorghasemi, K., Solmaz, H., Calam, A., & İpci, D. (2021). Effect of nitrogen and hydrogen addition on performance and emissions in reactivity controlled compression ignition. Fuel, 292, 120330.

[18] Singh, A. P., Kumar, V., & Agarwal, A. K. (2020). Evaluation of comparative engine combustion, performance and emission characteristics of low temperature combustion (PCCI and RCCI) modes. Applied Energy, 278, 115644.

[19] Han, X., Zheng, M., Tjong, J. S., & Li, T. (2015). Suitability study of n-butanol for enabling PCCI and HCCI and RCCI combustion on a high compression-ratio diesel engine (No. 2015-01-1816). SAE Technical Paper.

[20] Uyumaz, A., Aydoğan, B., Calam, A., Aksoy, F., & Yılmaz, E. (2020). The effects of diisopropyl ether on combustion, performance, emissions and operating range in a HCCI engine. Fuel, 265, 116919.

[21] Böğrek, A., Haşimoğlu, C., Calam, A., & Aydoğan, B. (2021). Effects of n-heptane/toluene/ethanol ternary fuel blends on combustion, operating range and emissions in premixed low temperature combustion. Fuel, 295, 120628.

[22] Amjad AK, Saray RK, Mahmoudi SMS, Rahimi A. Availability analysis of n-heptane and natural gas blends combustion in HCCI engines. Energy 2011;36(12):6900–9.

[23] Aydoğan, B. (2020). An experimental examination of the effects of n-hexane and n-heptane fuel blends on combustion, performance and emissions characteristics in a HCCI engine. Energy, 192, 116600.

[24] Polat, S., Solmaz, H., Uyumaz, A., Calam, A., Yılmaz, E., & Serdar Yucesu, H. (2020). An experimental research on the effects of negative valve overlap on performance and operating range in a homogeneous charge compression ignition engine with RON40 and RON60 fuels. Journal of Engineering for Gas Turbines and Power, 142(5), 051007.

[25] Bhaduri S, Jeanmart H, Contino F. EGR control on operation of a tar tolerant HCCI engine with simulated syngas from biomass. Appl Energy 2018;227:159–67.

[26] Calam A, Solmaz H, Yılmaz E, İçingür Y. Investigation of effect of compression ratio on combustion and exhaust emissions in A HCCI engine. Energy 2019;168:1208–16.

[27] Halis S, Nacak C, Solmaz H, Yilmaz E, Yucesu HS. Investigation of the effects of octane number on combustion characteristics and engine performance in a HCCI engine. J Therm Sci Technol 2018;38(2):73–84.

[28] Solmaz, H. (2020). A comparative study on the usage of fusel oil and reference fuels in an HCCI engine at different compression ratios. Fuel, 273, 117775.

[29] Yang R, Hariharan D, Zilg S, Mamalis S, Lawler B. Efficiency and emissions characteristics of an HCCI engine fueled by primary reference fuels. SAE Int J Engines 2018;11(6):993–1006.

[30] Zhou Y, Hariharan D, Yang R, Mamalis S, Lawler B. A predictive 0-D HCCI combustion model for ethanol, natural gas, gasoline, and primary reference fuel blends. Fuel 2019;237:658–75.

[31] Celebi, S., Haşimoğlu, C., Uyumaz, A., Halis, S., Calam, A., Solmaz, H., & Yılmaz, E. (2021). Operating range, combustion, performance and emissions of an HCCI engine fueled with naphtha. Fuel, 283, 118828.

[32] Atmanlı A, Yüksel B, Ileri E, Karaoglan AD. Response surface methodology based optimization of diesel–n-butanol–cotton oil ternary blend ratios to improve engine performance and exhaust emission characteristics. Energy Convers Manage 2015;90:383–94.

[33] Yusri IM, Majeed AA, Mamat R, Ghazali MF, Awad OI, Azmi WH. A review on the application of response surface method and artificial neural network in engine performance and exhaust emissions characteristics in alternative fuel. Renew Sustain Energy Rev 2018;90:665–86.

[34] Atmanli A, Ileri E, Yilmaz N. Optimization of diesel–butanol–vegetable oil blend ratios based on engine operating parameters. Energy 2016;96:569–80.

[35] Yatish KV, Lalithamba HS, Suresh R, Hebbar HH. Optimization of bauhinia variegata biodiesel production and its performance, combustion and emission study on diesel engine. Renewable Energy 2018;122:561–75.

[36] Simsek, S., & Uslu, S. (2020). Determination of a diesel engine operating parameters powered with canola, safflower and waste vegetable oil based biodiesel combination using response surface methodology (RSM). Fuel, 270, 117496.

[37] Ardebili, S. M. S., Solmaz, H., Calam, A., & İpci, D. (2021). Modelling of performance, emission, and combustion of an HCCI engine fueled with fusel oil-diethylether fuel blends as a renewable fuel. Fuel, 290, 120017.

[38] Babagiray M, Kocakulak T, Ardebili SMS, Calam A, Solmaz H. Optimization of operating conditions in a homogeneous charge compression ignition engine with variable compression. Int. J. Environ. Sci. Technol. 2022. https://doi.org/10.1007/s13762-022-04499-9.

[39] Kocakulak T, Babagiray M, Nacak Ç, Ardebili SMS, Calam A, Solmaz H. Multi objective optimization of HCCI combustion fuelled with fusel oil and n-heptane blends. Renewable Energy 2022;182:827–41.

[40] Simsek, S., Uslu, S., Simsek, H., & Uslu, G. (2021). Improving the combustion process by determining the optimum percentage of liquefied petroleum gas (LPG) via response surface methodology (RSM) in a spark ignition (SI) engine running on gasoline-LPG blends. Fuel Processing Technology, 221, 106947.

[41] Khanjani, A., & Sobati, M. A. (2021). Performance and emission of a diesel engine using different water/waste fish oil (WFO) biodiesel/diesel emulsion fuels:

Optimization of fuel formulation via response surface methodology (RSM). Fuel, 288, 119662.
[42] Srinidhi, C., Madhusudhan, A., Channapattana, S. V., Gawali, S. V., & Aithal, K. (2021). RSM based parameter optimization of CI engine fuelled with nickel oxide dosed Azadirachta indica methyl ester. Energy, 234, 121282.
[43] Babagiray M, Kocakulak T, Safieddin Ardebili SM, Solmaz H, Çınar C, Uyumaz A. Experimental and statistical investigation of different valve lifts on HCCI combustion, performance and exhaust emissions using response surface method. Energy 2022;244:123184.
[44] Chang J, Kalghatgi G, Amer A, Viollet Y. Enabling high efficiency direct injection engine with naphtha fuel through partially premixed charge compression ignition combustion. SAE Technical Paper; 2012. No. 2012–01-0677.
[45] Leermakers CAJ, Bakker PC, Somers LMT, De Goey LPH, Johansson BH. Commercial naphtha blends for partially premixed combustion. SAE Int J Fuels Lubr 2013;6(1):199–216.
[46] Viollet Y, Chang J, Kalghatgi G. Compression ratio and derived cetane number effects on gasoline compression ignition engine running with naphtha fuels. SAE Int J Fuels Lubr 2014;7(2):412–26.
[47] Chang J, Kalghatgi G, Amer A, Adomeit P, Rohs H, Heuser B. Vehicle demonstration of naphtha fuel achieving both high efficiency and drivability with EURO6 engine-out NOx emission. SAE Int J Engines 2013;6(1):101–19.
[48] Yılmaz E. A Comparative Study on the Usage of RON68 and Naphtha in an HCCI Engine. International Journal of Automotive Science and Technology 2020;4(2): 90–7.
[49] Uyumaz, A., Aydoğan, B., Yılmaz, E., Solmaz, H., Aksoy, F., Mutlu, İ., Calam, A. (2020). Experimental investigation on the combustion, performance and exhaust emission characteristics of poppy oil biodiesel-diesel dual fuel combustion in a CI engine. Fuel, 280, 118588.
[50] Arabacı E. Simulation and performance analysis of a spark ignition engine using gasoline and LPG as fuel. Journal of the Faculty of Engineering and Architecture of Gazi University 2021;36(1):447–57.
[51] Okcu, M., Fırat, M., Varol, Y., Altun, Ş., Kamışlı, F., Atila, O. (2022). Combustion of high carbon (C7-C8) alcohol fuels in a reactivity controlled compression ignition (RCCI) engine as low reactivity fuels and ANN approach to predict RCCI emissions. Fuel, 319, 123735.
[52] Figari, M., Theotokatos, G., Coraddu, A., Stoumpos, S., Mondella, T. (2022). Parametric investigation and optimal selection of the hybrid turbocharger system for a large marine four-stroke dual-fuel engine. Applied Thermal Engineering, 208, 117991.
[53] Liu, Y., Wang, X. J., Zhou, S., Chen, H. (2021). Enhancing public building energy efficiency using the response surface method: An optimal design approach. Environmental Impact Assessment Review, 87, 106548.
[54] Sharma, P., Chakradhar, D., Narendranath, S. (2021). Measurement of WEDM performance characteristics of aero-engine alloy using RSM-based TLBO algorithm. Measurement, 179, 109483.
[55] Ardebili, S. M. S., Babagiray, M., Aytav, E., Can, Ö., Boroiu, A. A. (2022). Multi-objective optimization of DI diesel engine performance and emission parameters fueled with Jet-A1–Diesel blends. Energy, 242, 122997.
[56] Özbek K, Özyurt Ö. Bina soğutma kapasitesine etki eden parametrelerin yanıt yüzey yöntemi (YYY) kullanılarak incelenmesi. Gümüşhane Üniversitesi Fen Bilimleri Dergisi 2022;12(1):309–19.
[57] Feng X, Liu Y, Li X, Liu H. RSM, ANN-GA and ANN-PSO modeling of SDBS removal from greywater in rural areas via Fe 2 O 3-coated volcanic rocks. RSC Adv 2022;12 (10):6265–78.
[58] Anani J, Noby H, Zkria A, Yoshitake T, ElKady M. Monothetic analysis and response surface methodology optimization of calcium alginate microcapsules characteristics. Polymers 2022;14(4):709.
[59] Myers RH, Montgomery DC, Anderson-Cook CM. Response surface methodology: process and product optimization using designed experiments. John Wiley & Sons; 2016.
[60] Torshizi, M. V., Azadbakht, M., Kashaninejad, M. (2020). Application of response surface method to energy and exergy analyses of the ohmic heating dryer for sour orange juice. Fuel, 278, 118261.
[61] Solmaz H, Ardebili SMS, Calam A, Yılmaz E, İpci D. Prediction of performance and exhaust emissions of a CI engine fueled with multi-wall carbon nanotube doped biodiesel-diesel blends using response surface method. Energy 2022;227:120518.
[62] Wang, H., Feng, B., Zhang, L., Li, Y., Zheng, Z., Yao, M. (2021). Experimental investigation on the effects of octane sensitivity on partially premixed low-temperature combustion. Fuel, 287, 119488.
[63] Chen, Y., Zhu, Z., Chen, Y., Huang, H., Zhu, Z., Lv, D., Guo, X. (2020). Study of injection pressure couple with EGR on combustion performance and emissions of natural gas-diesel dual-fuel engine. Fuel, 261, 116409.
[64] Balasubramanian, D., Wongwuttanasatian, T., Venugopal, I. P., Rajarajan, A. (2022). Exploration of combustion behavior in a compression ignition engine fuelled with low-viscous Pimpinella anisum and waste cooking oil biodiesel blends. Journal of Cleaner Production, 331, 129999.
[65] Calam, A. (2021) Homojen Dolgulu Sıkıştırma ile Ateşlemeli Bir Motorda N-Heptan-Tetrahidrofuran Karışımlarının Yanma, Performans Ve Emisyonlara Etkisi. Politeknik Dergisi. p. 1-1.
[66] Pintor DL, Gentz G, Dec J. Mixture stratification for CA50 control of LTGC engines with reactivity-enhanced and non-additized gasoline. SAE Technical Paper; 2021. No. 2021–01-0513.
[67] Wei, Z., Zhang, Y., Xia, Q., Liu, Y., Xu, Y. (2022). A simulation of ethanol substitution rate and EGR effect on combustion and emissions from a high-loaded diesel/ethanol dual-fuel engine. Fuel, 310, 122310.
[68] Zhang, Y., Xu, Y., Xia, Q., Liu, Y., Wei, Z., Sun, M. The effects of intake temperature on reactivity controlled compression ignition combustion under high load. Environmental Progress & Sustainable Energy, e13830.
[69] Rather MA, Wani MM. A numerical study on the effects of exhaust gas recirculation temperature on controlling combustion and emissions of a diesel engine running on HCCI combustion mode. International Journal of Automotive Science and Technology 2018;2(3):17–27.
[70] Polat S, Yücesu HS, Kannan K, Uyumaz A, Solmaz H, Shahbakhthi M. Experimental comparison of different injection timings in an HCCI engine fueled with n-heptane. International Journal of Automotive Science and Technology 2017;1(1):1–6.
[71] Khoa NX, Lim O. The Internal Residual Gas and Effective Release Energy of a Spark-Ignition Engine with Various Inlet Port-Bore Ratios and Full Load Condition. Energies 2021;14(13):3773.
[72] Mahla, S. K., Ardebili, S. M. S., Sharma, H., Dhir, A., Goga, G., & Solmaz, H. (2021). Determination and utilization of optimal diesel/n-butanol/biogas derivation for small utility dual fuel diesel engine. Fuel, 289, 119913.
[73] Ashour, M.K., Eldrainy, Y.A., and Elwardany, A.E. (2020) Effect of cracked naphtha/biodiesel/diesel blends on performance, combustion and emissions characteristics of compression ignition engine. Energy. 192: p. 116590.
[74] Calam TT, Çakıcı GT. A sensitive method for the determination of 4-aminophenol using an electrochemical sensor based on 5-amino-1, 3, 4-thiadiazole-2-thiol. Journal of Food Composition and Analysis 2022;114:104728. https://doi.org/10.1016/j.jfca.2022.104728.
[75] Calam TT, Çakıcı GT. Optimization of square wave voltammetry parameters by response surface methodology for the determination of Sunset yellow using an electrochemical sensor based on Purpald®. Food Chemistry 2023;404:134412. https://doi.org/10.1016/j.foodchem.2022.134412.
[76] Özer, S. and Vural, E. Pilot Yakıt Olarak Dizel/n-Heptan, Dizel/Toluen Kullanan Dizel Bir Motorda CNG İlavesinin Etkileri. Gazi Mühendislik Bilimleri Dergisi, 6(1), 1-15.
[77] Solmaz, H., Ardebili, S. M. S., Aksoy, F., Calam, A., Yılmaz, E., & Arslan, M. (2020). Optimization of the operating conditions of a beta-type rhombic drive stirling engine by using response surface method. Energy, 198, 117377.